Article

Dual Fluorophore containing efficient PET based molecular probe for selective detection of Cr3+ and PO43- ions through fluorescence “Turn–On–Off” response in partial aqueous and biological medium: Live cell imaging and Logic application

Sushil Kumar Dwivedi, Ramesh C. Gupta, Priyanka Srivastava, Priya Singh, Biplob Koch, Biswajit Maiti, and Arvind Misra

Anal. Chem., **Just Accepted Manuscript** • DOI: 10.1021/acs.analchem.8b02570 • Publication Date (Web): 14 Aug 2018

Dual Fluorophore containing efficient PET based molecular probe for selective detection of Cr^{3+} and PO_4^{3-} ions through fluorescence "*Turn–On–Off*" response in partial aqueous and biological medium: Live cell imaging and Logic application

Sushil K. Dwivedi[†], Ramesh C. Gupta[†], Priyanka Srivastava[†], Priya Singh[‡], Biplob Koch[‡], Biswajit Maiti[†] and Arvind Misra[†]*

[†]*Department of Chemistry, Institute of Science, Banaras Hindu University, Varanasi – 221 005 UP INDIA*

[‡]*Department of Zoology, Institute of Science, Banaras Hindu University, Varanasi –221005 UP INDIA*

Corresponding Author E-mail: *amisra@bhu.ac.in; arvindmisra2003@yahoo.com. Phone : +91-542-6702503; Fax: +91-0542-2368127, 2368175.*

Abstract

The present work describes a new PET based molecular probe in which naphthalimide (NPI) and anthracene (AN) chromophores are linked through a molecular bridge of piperazine and triazole units by Click reaction. A typical meaningful structural variation has made the present probe highly selective for Cr^{3+} ion (LOD, $5.567x10^{-8}$ M) that displayed enhanced, "turn – on" emission (due to PET–*Off* photophysical mechanism) and naked-eye sensitive bright green color fluorescence in the environment of interfering and competitive ions, in Tris-HCl buffer. The minimum energy structure obtained through theoretical calculations (DFT and TD-DFT) revealed a "tub" shape structure for probe **10**. Upon complexation the conformation of piperazine fragment change from *chair* to *boat* in which, the triazole and piperazine units create a cavity to tether Cr^{3+}. Moreover, the probe showed excellent biocompatibility and cell permeability to sense Cr^{3+} sensitively in live cell thus, holds great promise for application in biological and environment sciences. Additionally, the sensitive "*Off–On–Off*" sensing behavior of probe **10** providing two chemical inputs (Cr^{3+} and PO_4^{3-}) helps to construct an INHIBIT logic gate. Also the probe has been utilized as printing material to decode secret information through the Cr^{3+} ion containing "marker-ink" under UV light.

Introduction

Modern day research outcome encompasses very categorically about the vital role of metal ions in many fundamental biological processes. In living organism the transition metal ions are generally present in trace amount and often serve as important cofactors in diverse enzymatic and redox reactions. A slight disturbance in metal ion homeostasis may lead to acute and long-term diseases, including heart disease, cancer and neurodegeneration.[1] Specifically, the trivalent metal ions such as, Fe^{3+}, Al^{3+}, Cr^{3+} have their own biological importance and are directly involved in the cell functions where there is a critical control of M^{3+} levels.[2,3] Among them, the chromium ions (Cr^{3+}) (recommended daily intake for an adult; 50-200mg)[4] help to activate certain enzymes and stabilizing factors associated with important biological events like, metabolism of carbohydrate, fat, protein and nucleic acids.[5-9] The deficiency of Cr^{3+} may impair immune function and also increase the chance of diabetes and cardiovascular disease by influencing the level of circulating insulin, glucose, triglycerides, and total cholesterol.[10] The mechanism by which Cr^{3+} affects human metabolism is based on modulation in insulin action through glucose tolerance factors (GTF).[11-13] Moreover, the excess of Cr^{3+} is carcinogenic.[14] At elevated temperature Cr^{3+} binds with DNA and make an adverse change in cellular structure or even damage the cellular components to cause mutation and cancer.[15,16] Cr^{3+} oxidizes to more toxic Cr(VI) that can easily penetrate cell membrane and if ingested in excess death of an organism is possible due to oxidization of DNA and some proteins.[17,18]

Moreover, metallic chromium or its compounds have wide industrial applications such as, chromo-plating, leather tanning, batteries, anodizing operation, dye, paint, welding, corrosion, wood preservative etc. therefore, industrial runoff of Cr^{3+} is on high risk of severe environment pollution.[19,20] The chromium content in natural water is normally at μgL^{-1} level and there are

severe matrix interference which cannot be minimized.[21] The direct sensitive determination of chromium in water is costly and involve expensive analytical methods.[5,22,23] Thus, the recognition of ions is important in the area of supramolecular chemistry and chemical sensor technology and fluorescence spectroscopy is the simplest and cost effective tool to achieve information of such events in real time. [24,25]

A limited number of molecular probes are known for selective and quantitative detection of Cr^{3+}.[26] However, most of them worked on fluorescence "turn-off" strategy because paramagnetic Cr^{3+} is known to induce strong fluorescent quenching. Till today only few probes are explored to monitor Cr^{3+} in solution and live cells through fluorescence "turn-on" response.[27-28] Nam *et.al*[29] utilized cyclometalated Ir(III) complex to detect Cr^{3+} through modulation in PET and ILCT processes. Duan *et.al*[30] reported dansyl derivatives for Cr^{3+} ion. Li *et. al*[31,32] reported some rhodamine derivatives to detect Cr^{3+} in solution and live cells. Similarly, some naphthalimide derivatives have been developed for Cr^{3+} ions with some limitations.[13, 33-35] Thus, there is a great need of some sensitive chemosensors to monitor Cr^{3+} selectively in environment and biological samples.

Therefore, motivated with the challenges and our ongoing research interest in the design of some smart scaffolds for selective detection of biologically important species, we deepen our interest to develop an efficient probe for recognition of Cr^{3+}. To have an efficient sensor probe the structural motif, choice of chromophore and ionophore and/or binding site are crucial. For instance, we previously reported some molecular probes based dansyl, benzhydryl-anthracene and thiophenyl-naphthalimide chromophores[36-38] in which, *N* atoms of flexible piperazine unit and other coordination sites in the form of *O* and *S* atoms could able to tether the metal ions like, Hg^{2+} and Fe^{3+} effectively. In continuation to that, the present work describes a new probe in

which NPI and AN units are linked through a slightly rigid piperazine-triazole molecular bridge by Click reaction. The typical structural modification notably made the present probe PET sensitive that could detect Cr^{3+} ion selectively in solution and live cell without interference of biologically important competing metal ions such as, Hg^{2+}, Fe^{3+}, Cd^{2+}, Ni^{2+}, Co^{2+}, Al^{3+}.

Experimental Section:

Sample preparation: In pure water probe **10** is partially soluble but the optimum solubility of the probe was found in 60% aqueous-THF, v/v = 4:6. Therefore, for photophysical studies the stock solution of probe (c = 1 x 10^{-3} M) was prepared in tetrahydrofuran (THF). Then, the 15 µL of stock solution was diluted in Tris-HCl buffer (5.0 µM; 60% aqueous THF, v/v = 4:6; pH, 7.2) to make the final concentration 5 µM in a 3 mL solution. For metal ion interaction studies 0.1 M solution of different ions were used. For ^{1}H NMR titration experiment the solution of probe (c = 1 x 10^{-2} M) and $Cr(NO_3)_3$ were prepared in $CDCl_3$. All the measurements including biological and live cell studies have been performed in THF/Tris-HCl buffer (THF:H_2O, v/v 4:6; pH, 7.2) gradient system.

Estimation of LOD: The calibration curve was obtained by diluting probe solution (2 µM) to 0.10 µM concentration and emission spectra acquired in the concentration range 0.9 to 0.1 µM. To estimate calibration sensitivity (m) fluorescence plot was obtained between ($I - I_0$) (where I_0 and I are intensities of probe in the presence and absence of Cr^{3+}) and Cr^{3+} ion concentrations. From the slope of fluorescence curve the calibration sensitivity (m) was estimated.

Quantum Chemical calculations: The geometry optimization and quantum chemical calculations of probe **10** and their probable complex, **10.Cr^{3+}** were performed by density functional theory (DFT) method as implemented in Gaussian 03 suits of program employing basis set B3LYP/6-31G* and for metal ion B3LYP/LANL2DZ* respectively. A frequency

calculation for the metal complex was performed to make sure that the optimized structure is a real minimum. The quantum chemical calculations using the time-dependent density functional theory (TD-DFT; specifically, uB3LYP TD-FC/6-31G (d, p)) have been performed using GAUSSIAN 09 suits of program.

MTT Assay: Human cervical cancer cell line (HeLa) was cultured in 25-cm^2 flask at 37˚C in a humid incubator under 5% CO_2 environment. The cells were grown in Dulbecco's modified Eagle's medium (DMEM) containing 10% FBS, penicillin, and streptomycin. To maintain exponential growth cells were split when reached at 80% confluency. Prior to exposure to probe HeLa cells were seeded in a 96-well plate ($1x10^5$ cells per well) and incubated for 24h for complete adherence. After that cells were incubated with different concentration of probe **10** (0, 5, 10, 50, 100, 150, 200 µM) for 24h. Then, MTT solution (100 µL; 5 mg/mL in PBS) was added into each well. After incubation for 2h the residue was treated with DMSO (100 µL) to dissolve purple color formazan crystals. The absorbance was recorded on a micro plate reader at 570 nm and the percentage of cell viability was estimated [Cell viability (%) = Absorbance of detection group / Absorbance of control group x 100%].

Cell imaging: The cultured HeLa cells were seeded in cultured 12 well plate and left for overnight incubation as per standard protocol. Next, live cells were incubated with the probe **10** (25 µM and 50 µM) for 24h and 48h and after washing with PBS buffer (2 times) images were acquired under blue and green channels. For ion interaction studies probe **10** treated cells were incubated with Cr^{3+} ion (25µM) for 30 min. Similarly, cells containing **10**.Cr^{3+} were incubated with PO_4^{3-} anion (50 µM) for 30 min. All the cell images were taken under fluorescence microscope.

Results and Discussion:

Probe Design and photophysical studies: For an efficient sensory behavior application of homo or hetero bireceptor type dyad or triad systems are more advantageous to get significant output signals upon interaction with an ion.[39,40] The present system is like a heterobifluorophoric format [$Fluorophore_1$-$Spacer_1$-$Receptor_1$-$Spacer_2$-$Receptor_2$-$Fluorophore_2$] in which we can apply two separate excitation wavelength. One is suppose to give an ion sensitive fluorescence (NPI unit, sensory) while the other one remain insensitive to ion concentration (ion-invariant). The ion invariant (AN unit) component is expected to serve as an internal reference. The designed organic supramolecular assembly is interesting because the possible photophysical mechanism like, photoinduced electron transfer (PET) or intramolecular electron transfer (intra-ELT) and electronic energy transfer (intra-EET) due to short range interactions, are likely to play their important role.[41]

The synthetic route adopted for the preparation of probe **10** is shown in Scheme-1. A widely applicable "Click Chemistry" has been explored to promote cycloaddition reaction[42] between terminal alkyne containing NPI derivative, **5** and anthracene azide, **9** in presence of $CuSO_4$ as a catalyst in DMSO-H_2O (5.0 ml, 4:1 v/v). The rigid triazole-piperazine (tertiary amine) molecular bridge has been utilized as a suitable ionophore site to bind metal ions. In the sequence of reactions, naphthalic anhydride was first subjected to bromination and then refluxed with methylamine in methanol to get compound **3**. Compound **3** and **4** were refluxed in pyridine to get compound **5** in good yield. Moreover, anthracene carboxaldehyde was first reduced with $NaBH_4$ in methanol then treated with thionyl chloride to get synthon **8** in good yield. Compound **8** was further treated with sodium azide to get 9-azidomethylanthracene, **9**. The synthesized compound

were purified by column chromatography and characterized by $^{1}H/^{13}C$ NMR, FTIR and HRMS spectroscopic data. (Please see supporting information and Figure S1-17).

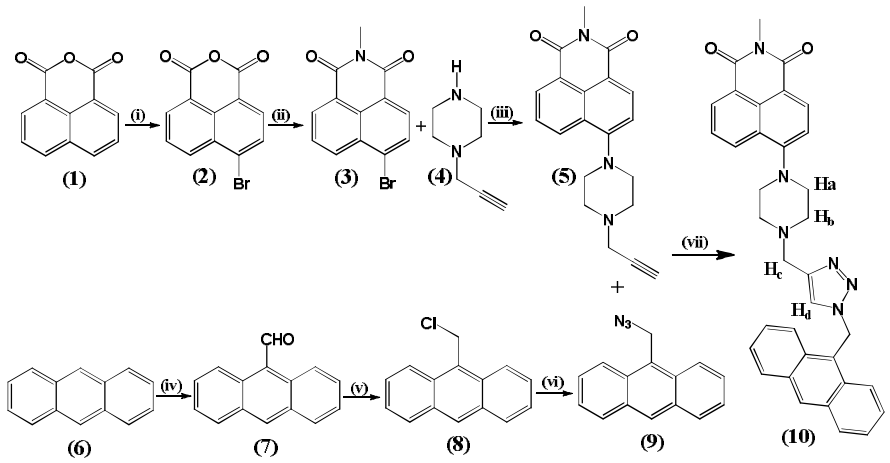

Scheme1: (i) KOH/Br_2 **(ii)** $CH_3OH/CH_3NH_2/60^oC$ **(iii)** Pyridine/TEA/100^oC **(iv)** $POCl_3$/DMF/80^oC **(v)** MeOH/$NaBH_4$/0^oC/$SOCl_2$/DCM/0^oC **(vi)** NaN_3/DMF/80^oC **(vii)** DMSO/H_2O/$CuSO_4$/sodium ascorbate.

Response probe 10 toward metal ions: First we optimized the compatibility of the probe in the solvent of different polarities. The absorption spectrum of molecular probe **10** (5 μM) in solvent systems such as, hexane, benzene, 1,4-dioxane, THF, methanol, chloroform, DMSO, and acetonitrile do not show any significant modulation in structured bands (Figure S18a). In 60% aqueous THF medium the observed low energy broad absorption band at ~ 410 nm correspond to naphthalimide (NPI) unit while typical anthracene (AN) absorption bands appeared at ~ 387, 366 and 347 nm (Figure S18a). However, the normalized emission spectra of probe **10** in different solvents displayed shift in ICT band toward longer wavelength e.g. $\lambda_{em.}$ = 475 nm (hexane), 527 nm (MeOH), 529 nm (THF: H_2O 40:60 v/v) (Figure S18b) region along with inconsistent variation in Stokes shift and quantum yield (Table S1). This could be ascribed to interaction of probe with solvents of different polarity and polarizability. In a preliminary experiment we first screened the fluorogenic affinity of probe toward different metal ions in different solvents. Interestingly, the emission feature of probe **10** in solvents like, THF, MeOH and DMSO showed

inexplicable behavior with different metal ions. However, selectivity of probe **10** for Cr^{3+} was relatively high (Figure S19). Knowing the fact that chromium metal interacts with water molecule to form corresponding hydrates and hydroxides and reduces the pH of the medium below ≤ 5.[1] To avoid the extent of hydrolysis of Cr^{3+} and to inhibit pH drop photophysical behavior of the probe in the absence and presence of metal ions were examined in the Tris buffer solution (5.0 μM; 60% aqueous THF, v/v = 4:6; pH, 7.2) (Figure 1).

The electronic transition spectrum of probe **10** showed high energy anthracene (AN) absorption bands at 352 nm, 367 nm and 387 nm while the low energy naphthalimide (NPI) broad absorption band appeared at ~ 410 nm (Figure 1, S20a). Upon providing excitation energy corresponding to AN band (at 387 nm) probe **10** (5.0 μM) displayed a weak broad emission band at 529 nm ($\Phi_{\mathbf{10}}$= 0.03) along with very weak AN emission band at 410 nm. This could be attributed to photoinduced electron transfer (PET) and/or intramolecular electronic energy transfer (EET) process (Figure S21). Upon interaction with different metal ions probe **10** revealed relatively high affinity for Cr^{3+} ion wherein, the low energy absorption bands disappeared and the molar absorptivity of high energy band increased. Similarly, upon interaction with Cr^{3+} (5.0 equiv) the weak emission band of probe **10** centered, at 529 nm displayed enhanced emission, "turn-on" with a blue shift of 14 nm and the quantum yield of the probe ($\Phi_{\mathbf{10}}$= 0.03) increased by ~11 fold ($\Phi_{\mathbf{10}}$ = 0.34). And a bright green color fluorescence (*switched – On*) appeared in the medium. However, the other tested metal ions such as, Na^{+}, K^{+}, Ca^{2+}, Mg^{2+}, Co^{2+}, Ni^{2+}, Zn^{2+}, Fe^{2+}, Pb^{2+}, Cd^{2+}, Fe^{3+} and Hg^{2+} failed to exhibit any considerable change in the color and photophysical behavior of the probe (Figure 1). The observed considerable enhancement in the relative fluorescence intensity of probe **10** with Cr^{3+} may be attributed to suppression of PET process. It is noteworthy to mention that PET process generally

involves *Off-On* or *On-Off* switching behavior without any considerable wavelength shift. In probe **10** AN unit (ion-invariant) was chosen as first fluorophore (Fl_1) in which triazole (Rec_1) and piperazine (Rec_2) receptor fragments are connected through methylene spacers (Spr_1 and Spr_2). The second fluorophore NPI was considered as a sensory unit. The tertiary amine function (connected with triazole) of piperazine unit is involved in intramolecular PET whereas the 4-amino function (tertiary) of NPI unit is responsible for internal charge transfer (ICT) process through the lowest energy singlet excited state. Therefore, the observed blue shift of 14 nm, upon interaction with Cr^{3+} ion, is attributed to inhibition in ICT process. Moreover, the normalized emission and absorption spectra revealed that emission of AN unit (at λex. = 386 nm) is completely merged within the absorption bands of NPI derivative 5 (Figure S20b). The excitation spectra (at λex.= 529 nm) of probe **10** was found almost similar to absorption spectra and upon interaction with Cr^{3+} (Figure S22a) or below pH, $\leq$6 (Figure S22c) the broad band of NPI unit diminished while the intensity of AN unit enhanced successively. Further, the excitation spectra at 410 nm also suggested about the energy transfer from AN to NPI moiety (Figure S22b). Thus, it is noteworthy to mention that due to some extent of rigidity around molecular bridge electronic energy transfer from S_1 state of AN to NPI either through space or bond interaction, is very much possible via intra-EET process along with conventional PET in which, naphthalimide emission dominate.[39-41,43]

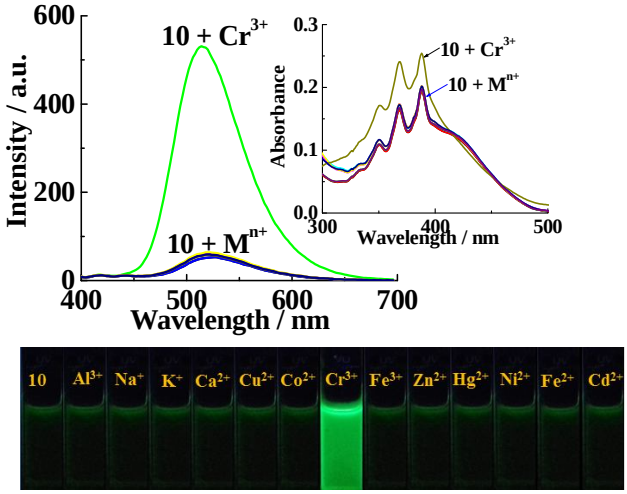

Figure 1: Emission and in inset absorption spectra of probe **10** (5.0 μM) upon interaction with different metal ions in THF/Tris-HCl buffer (THF:H_2O, v/v 4:6; pH, 7.2). **Image:** Naked-eye sensitive fluorogenic response of probe **10** in the presence of tested metal ions (under UV light; at 365 nm).

The high selectivity of probe **10** for Cr^{3+} ion was assessed by interference studies. Upon addition of competitive metal ions (in excess) to a solution of a probable complex, **10.Cr^{3+}** or reversibly, addition of Cr^{3+} to the solution of **10.M^{n+}** insignificant change was observed in the both absorption and emission spectra (Figure S23, S24). Metal ions like Cu^{2+} and Cr^{3+} are known to induce fluorescence quenching however, present structural motif displayed "turn–on" emission with Cr^{3+} even in the presence Cu^{2+} ion in the medium (Figure S25). Further, to examine the reversibility in complexation the complex, **10.Cr^{3+}** was treated with a strong chelating ligand, EDTA. Upon addition of excess of EDTA (20 equiv) the intensity of the complex, **10.Cr^{3+}** diminished. Further addition of Cr^{3+} to the same solution regained the intensity of probe. We could repeat this process for about eight cycles, and found that the emission behavior of probe remained consistent without any significant loss in relative fluorescence intensity (Figure S26). Thus, suggesting about the extraction of Cr^{3+} from its complex, **10.Cr^{3+}**.

Further to understand exact stoichiometry for interaction between probe **10** and Cr^{3+} ion titration experiment was performed. Upon a gradual increment of Cr^{3+} ions (0-5 equiv) to a solution of probe **10** the relative intensity centered, at 529 nm (*switched–Off* state) enhanced, "turn-on" significantly (~ 93–94%) with a blue shift of ~ 14 nm (Figure 2) and a bright green color fluorescence appeared (*switched–On*) in the medium. Similarly, the absorption spectra of probe **10** displayed rise in molar extinction coefficient upon increasing the concentration of Cr^{3+} ion (Figure S27).

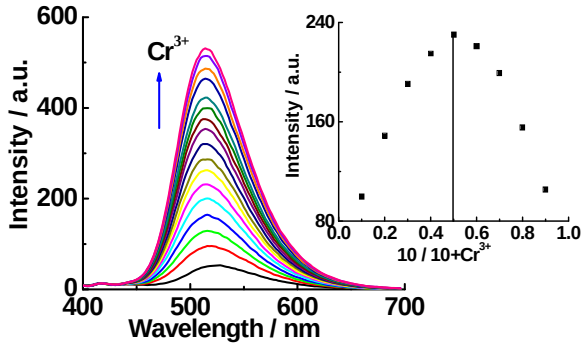

Figure 2: Emission titration spectra of probe **10** (5.0 μM) with Cr^{3+} (5 equiv) in THF/Tris-HCl buffer (THF:H_2O, v/v 4:6; pH 7.2). Inset: Job's plot based on emission titration data.

Job's plot analysis based on emission spectral data suggested about a 1:1 stoichiometry (Figure 2, inset) for which the binding constant was estimated using Benesi-Hildebrand (B-H) method[44] and was found to be K_{ass}= 5.87x10^5 M^{-1} (Figure S28). In order to estimate the limit of detection (LOD) for Cr^{3+} a calibration curve was obtained. An almost straight line calibration curve with standard deviation (σ) 0.03203 suggested about a linear correlation between intensity and concentration of probe **10** (Figure S29a). The slope of fluorescence curve gave the calibration sensitivity (*m*) 59.436 (Figure S29b) in the aforementioned range. The estimated limit of

detection (LOD = $\mathbf{3\sigma/m}$) 5.567×10^{-8} M was found comparable to some other reported methods (Table S2).

***pH sensitivity*:** The probe **10** contains piperazine unit and is sensitive to pH of the medium. Secondly, the availability of Cr(III) ions in the medium is also pH dependent (pH, 5.2–8.3).[25,47] Therefore, we examined the pH dependent photophysical behavior of probe **10**. Notably, the probe **10** displayed insensitive behavior between pH 7 to 14. However, under acidic condition the molar absorptivity corresponding to anthracene bands increased while the NPI broad band gets diminished (Figure S30). However, the intensity of probe enhanced significantly (~33% between pH ~ 5.0 to 6.0, and ~ 91% between pH ~ 4.0 to 1.0) (Figure 3, and S22c) due to the protonation of the *N* atoms of piperazine unit (pH < 5.0) consequently, suppressing the PET (PET-*Off*) from piperazine to naphthalimide unit. Further, the pH-dependent emission spectra of probable complex, **10**+Cr^{3+} remained insensitive to pH variations (1 to 14) (Figure 3, inset). Since, below pH ≤5.0 quaternary ammonium salt is formed therefore no coordination sites are available to tether Cr^{3+} ion. Thus, the distribution of probe **10** in a broad pH range has suggested applicability of probe to detect Cr^{3+} under physiological pH (pH 7.0) condition and biological medium.

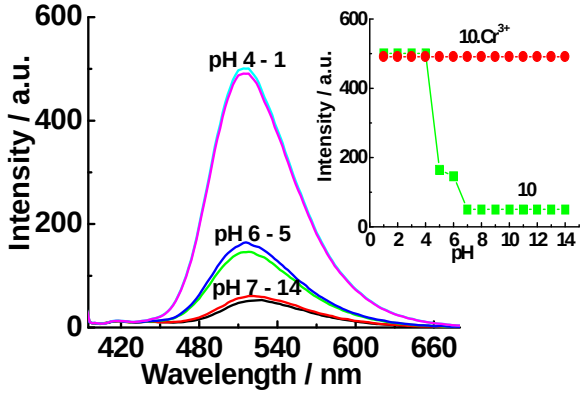

Figure 3: Change in emission spectra of probe **10** (5μM) at different pH in THF/Tris-HCl buffer (THF:H_2O, v/v 4:6; pH, 7.2). Inset: Shows change in emission behavior of probe **10** its complex **10**.Cr^{3+}.

Response of probe 10 toward Anions: In order to understand the affinity of probe **10** for different class of anions such as, F^-, Cl^-, Br^-, I^-, AcO^-, CN^-, N_3^-, CO_3^{2-}, HSO_4^-, NO_3^- and PO_4^{3-} the absorption and emission spectra were acquired under similar experimental condition. Notably, the probe **10** showed insignificant behavior toward the tested anions (Figure S31). Next, we examined the affinity of a probable complex **10**.Cr^{3+} with tested anions (~20.0 equiv). Notably, the emission intensity of the probe **10** revived upon interaction with PO_4^{3-} anion while remained silent toward other tested anions (Figure 7c, and S32b). This may be attributed to displacement of Cr^{3+} from its probable complex, **10**.Cr^{3+}. To know the equivalent of PO_4^{3-} anion required to displace Cr^{3+} from its complex titration experiment was performed (Figure S33a). It is interesting to mention that upon a gradual addition of PO_4^{3-} (0-20equiv) the enhanced emission of complex, **10**.Cr^{3+} diminished gradually probably due to release of Cr^{3+} ion in the medium and color of the solution reached to a *switched–Off* state. Further addition of Cr^{3+} to a solution of **10.**$\mathbf{Cr^{3+}}$**+**$\mathbf{PO_4^{3-}}$ the emission intensity regained and was almost similar to the intensity of a complex **10**.Cr^{3+}. On repetition of this process for about eight cycles we observed simultaneous decrease and increase in the relative intensity of the probe (*switch–Off–On*) without

any considerable loss in intensity and color of the solution (Figure S33b). This clearly indicated about the reversible mode of sensing with Cr^{3+} and PO_4^{3-} ions. To make sure about high selectivity of the complex, **10**.Cr^{3+} for PO_4^{3-} ion studies have been performed with ATP, ADP, and PPi. The emission behavior of **10**.Cr^{3+} revealed insignificant sensitivity for ATP and ADP while about a small fluorescence quenching (9%) occurred with PPi (Figure S34). Moreover, the estimated limit of detection of the complex, **10**.Cr^{3+} for PO_4^{3-} anion was found to be 3.90 x 10^{-7} M (Figure S29c). In order to understand the extent of fluorescence quenching with PO_4^{3-} anion, quenching constant (K_{sv}) was estimated from an almost linear Stern-Volmer plot (R^2 = 0.9979) and was found to be 5.87x10^5 M^{-1} (Figure S35). Thus, the probe **10** could serve as a potential reusable "*PET–Off –On*" chemosensor for Cr^{3+} and PO_4^{3-} ions in the studied medium. Furthermore, the fluorescence life time (τ) studies have been performed to rationalize the sensing mechanism (Figure S36). Interestingly, upon interaction with chromium (**10**.Cr^{3+}) the faster decay components (A1) of probe **10** (31.71%) decreased (24.81%) while the longer decay component value (A2) increased (75.19%) (Table S3). Similarly, upon interaction of **10**.Cr^{3+} with PO_4^{3-} the faster and longer decay components of **10**.Cr^{3+} were respectively increased (36.12%) and decreased (63.88%). Moreover, the decay time of probe **10** (4.7184 ns), based on double exponential decay fittings, increase and decrease for the species **10**.Cr^{3+} (5.6164ns) and **10**.Cr^{3+}+PO_4^{3-} (4.3330ns) respectively. Thus, TRPL studies also corroborate fluorescence "turn-*On-Off*" sensing mechanism with respective ions.

Mechanism of Interaction with Cr^{3+}:

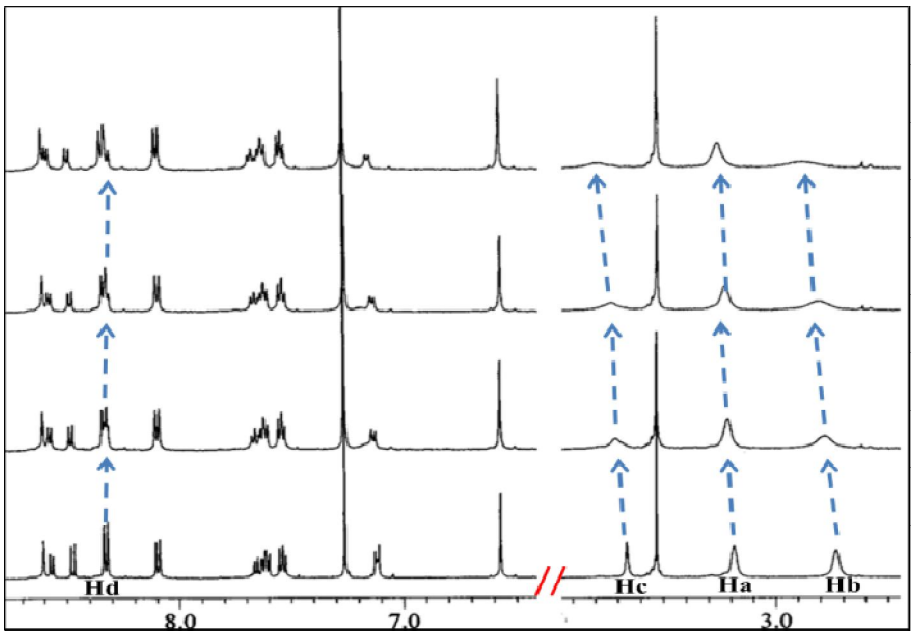

Figure 4: Stacked ^{1}H NMR spectra of probe **10** (2.0 x 10^{-2} M) upon addition of Cr^{3+} ions (0-2.0 equiv.) in $CDCl_3$.

^{1}H NMR titration studies: To gain a deep insight about the actual mode of interaction between probe **10** and Cr^{3+} ion ^{1}H NMR titration experiments were performed in $CDCl_3$. Upon interaction with Cr^{3+} (0-2.0 equiv) the resonances corresponding to piperazine and methylene protons, H_a (δ 3.18, s), H_b (δ 2.73, s) and H_c (δ 3.52, s) broadened and exhibited downfield shift (Δδ = 0.21, Δδ = 0.08 and Δδ = 0.15 ppm) respectively, while H_d proton (δ 8.31, merged with AN protons) of triazole ring exhibited a narrow upfield shift (Figure 4). Moreover, in the FT-IR spectra the typical C-N function stretching vibration bands (1286, 1231, 1039, 1020 cm^{-1}) upon interaction with Cr^{3+} shifted upfield to appear at 1283, 1229, 1039, 1006 cm^{-1} respectively (Figure S12). Additionally, in HRMS the molecular ion peak of probe **10** appeared at *m/z* 567.2485 (**10**+H^{+}; calc. 566.2430) while upon complexation with Cr^{3+} a new peak appeared at *m/z* 806.1810 (calc. 804.1470) (Figure S13-14). Thus, ^{1}HNMR, FTIR and HRMS studies clearly supported about the binding of probe with Cr^{3+} through *N* atoms of piperazine-triazole molecular bridge in 1:1 stoichiometry.

DFT/TD-DFT Studies: The DFT optimized minimum energy structure (Figure S37) also revealed that probe interacts with Cr^{3+} through the *N* atoms of piperazine-triazole bridge with bond lengths 2.09, 2.10 and 2.08 Å. The distance between NPI and AN units is found to be 10.47Å. The minimum energy structure revealed *chair* conformation for piperazine in which NPI and triazole linked AN units occupy equatorial (*1,4*) positions. The vertically placed two chromophoric units are almost perpendicular to each other and provide a virtual "tub" shape structure. Upon complexation with Cr^{3+} the piperazine unit rearranges to attain *boat* conformation wherein both triazole and piperazine units come close to each other. Thus, a cavity like structure generated to tether Cr^{3+} ion successfully, while the distance between the two chromophores increased to ~ 12.84Å. The frontier molecular orbital diagram suggested that the electron density in HOMO is mainly localized over NPI and piperazine units while in LUMO electrons are mainly localized on AN moiety, with energy difference (ΔE) about 1.8912 eV (Figure S38). Whereas, in case of **10**.Cr^{3+} the maximum electron density resides on HOMO of NPI and LUMO of AN moieties, with energy difference (ΔE) 0.0239eV. In order to understand the PET mechanism the TD-DFT calculations were performed and the relevant MOs of **10** and its complex **10**.Cr^{3+} were analyzed (Figure 5 and S39). It has been found that the energy (-5.49996eV) associated with HOMO of **10** reduced (-13.29167eV) significantly upon complexation with Cr^{3+} consequently, restricting the PET. It is important to mention that, for **10** most favorable electronic transition (Table S4) occurred from HOMO to LUMO+1 (ΔE, 3.43027eV) in which the electron density of piperazine unit is partially transferred to NPI unit (PET–*ON*). In contrast, for a complex **10**.Cr^{3+} the most favorable transition occurred from HOMO-4 to LUMO+1 (ΔE, 4.09857eV) wherein, the electron density of NPI-piperazine fragment remained toward metal centre (PET-*Off*) (Figure 5). A significant decrease in the

energy of HOMO (ΔE, ~8.95336eV) also suggested about the involvement of EET process either through electron exchange or emission-reabsorption.[39]

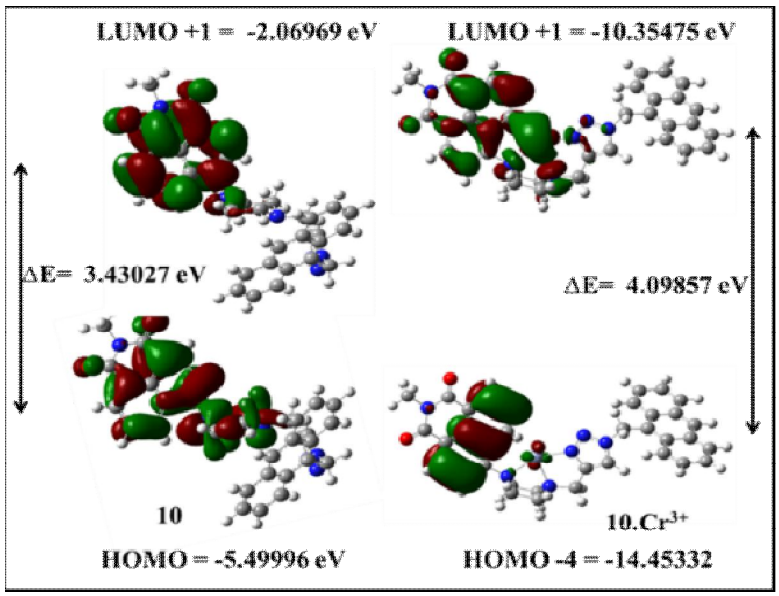

Figure 5: Excited state DFT optimized HOMO-LUMO energy distribution for **10** and its complex, **10**.Cr^{3+}.

Studies of Probe 10 in biological medium:

Encouraged by the observed high affinity of probe **10** to detect Cr^{3+} ion selectively in a buffer solution (pH, 7.2) we further intended to examine the photophysical behavior of probe and its affinity for Cr^{3+} ion in biological medium. In the protein medium (bovine serum albumin, BSA) upon providing high excitation energy (λex = 278 nm due to tryptophan residues of BSA) both probe **10** and its complex, **10**.Cr^{3+} could not able to display any considerable change and remained independent to even high concentration of BSA (3μM) (Figure S40). Moreover, probe **10** in the presence of BSA (10.0 equiv.) showed high affinity for Cr^{3+} with enhanced, "turn–*On*" emission, almost similar to the emission observed without BSA. It clearly indicated about negligible chance of possible nonbonding, electrostatic and H-bonding interactions and even with electrolytes present in blood serum.

Live cell imaging: Prior to live cell imaging the effect of probe on the viable HeLa cells was examined by tetrazolium (MTT) assay based on the action of mitochondrial dehydrogenase enzyme and calorimetric measurement.[37] The MTT assay suggested that probe can easily permeate into HeLa cells with good cytocompatibility (Figure S41) as the 70 to 80% cells were viable at 100µM to 200µM concentration of probe. For cell imaging the probe **10** (25 µM and 50 µM) incubated HeLa cells were visualized under blue and green channels. However, insignificant intracellular fluorescence was observed (Figure 6b and S42b). Whereas when the probe incubated HeLa cells were incubated with Cr^{3+} (25 µM) for 30 min a bright green fluorescence, "*turn–On*" appeared (Figure 6c). This clearly shows the compatibility of probe to monitor the Cr^{3+} ions intracellularly. It is important to mention that in solution around pH 5 the relative intensity of probe marginally increases (10-15%) while the probe incubated cells do not show any considerable intracellular fluorescence. A long term retention studies have been performed to assess the extent of intracellular retention of probe. The images of probe (25 µM) loaded HeLa cells showed insignificant fluorescence even after 24h and 48h incubation (Figure S43). Thus, the probability of interaction with the lysosomes was almost negligible and we could observe the green fluorescence only in the presence of Cr^{3+}. The cell imaging experiments were repeated to understand the fluorescence "*On–Off*" switching behavior in the presence of Cr^{3+} and PO_4^{3-} ions, intracellularly. Interestingly the observed bright green fluorescence of **10**.Cr^{3+} diminished (switched–*Off*) after interaction with PO_4^{3-} ions (Figure 6d).

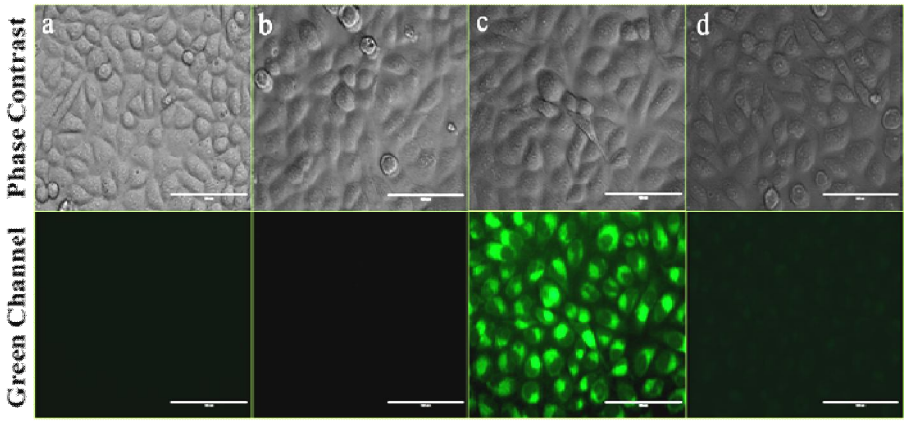

Figure 6: Fluorescence imaging in HeLa cells (a) Control and with (b) probe **10** (25 µM) (c) probe **10**+Cr^{3+} (25 µM) (d) **10.Cr^{3+}** and PO_4^{3-} (50 µM).

***Off-On* switching behavior and Logic implication:** Numerous chemically driven molecular switches can be derived from the unique modulation in optical signature of chemosensors incur upon interaction with important guest species. The present molecular assembly remains in switched–*On* state in the presence of Cr^{3+} (output; green fluorescence) while in switched–*Off* state (diminished emission) in the absence of Cr^{3+} and upon interaction of **10+Cr^{3+}** with PO_4^{3-} anion. Thus, the observed emission behavior correlates the "*Off-On-Off*" switching mechanism and has been realized to construct a logic gate by applying two chemical inputs as, *In*1 (Cr^{3+}) and *In*2 (PO_4^{3-}). According to the truth table (Figure 7b) sequential logic operations **10+Cr^{3+}** displayed high output emission (threshold value ~70%; at 515 a.u.) whereas, low output emission was obtained when the applied logic inputs were **10**, **10+PO$_4^{3-}$**, **10+Cr^{3+}+PO$_4^{3-}$** respectively. Thus, the truth table corresponds to a combinational (consisting of a NOT and an AND gate) INHIBIT logic gate (Figure 7a).

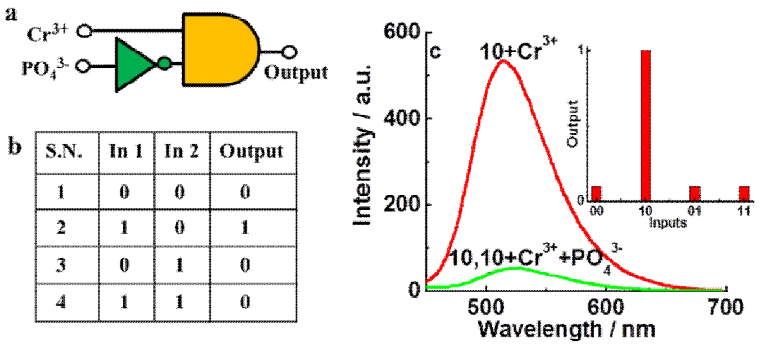

S.N.	In 1	In 2	Output
1	0	0	0
2	1	0	1
3	0	1	0
4	1	1	0

Figure 7: (a) INHIBIT logic gate with two inputs, *In*1 (Cr^{3+}) and *In*2 (PO_4^{3-}) (b) Truth table (1 = On; 0 = Off states) (c) Emission spectra and Bar diagram show output signals of probe **10** corresponding to inputs**,** **10**.Cr^{3+}, **10**.PO_4^{3-} and **10**.Cr^{3+}+PO_4^{3-}.

Application of probe in Press-Jet Printing: An attempt was made to explore the real time fluorescence response of probe **10** as a potential press-jet printing material. The printing papers were prepared by simply dipping cellulose paper (Whatman^{TM}) into a solution of probe **10** (2mM) in THF for 5 min and then washed with PBS buffer and dried in air. A very weak fluorescence (at 365nm) suggested the adsorption of probe **10** on cellulose paper (Figure 8a). A secret code, "BHU" was written with Cr^{3+} solution as a "marker ink" (2×10^{-3} M). Upon exposure of UV light (at 365 nm) a high-definition image was appeared (Figure 8c) while in normal light (control) no such images were observed (Figure 8b). The stability of image on the paper was good and no photo-bleaching occurred for more than 14 days at room temperature. Thus, the probe loaded papers afford great promise in hiding and sending the information secretly. Moreover, to know the reversibility and reusability of tested paper washing was done with phosphate buffer ($2x10^{-2}$ M) for several times. Insignificant loss in the intensity of image of secret code shows one time use of such material.

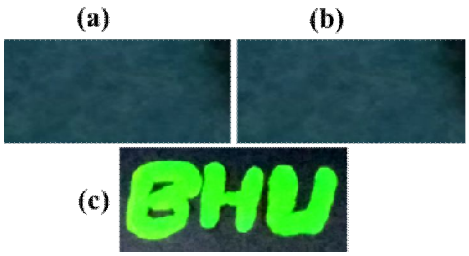

Figure 8: Image of press-jet printing sheet with Probe **10**. Decoding of Secret code, "BHU" written with Cr^{3+} containing "marker ink" under (**b**) visible light and (**c**) UV light (at 365 nm).

Conclusion:

In summary, we have developed a new efficient PET based molecular probe for a selective detection of Cr^{3+} in solution and biological medium. The probe **10** upon interaction with chromium ion selectively, displayed enhanced emission, fluorescence "turn–On" response. The bright fluorescent green color appeared in the medium was sensitive to the naked-eyes. The molecular probe has shown good detection limit and stability in wide pH range. The excellent biocompatibility of probe holds great promise for selective detection of Cr^{3+} in biological medium and environment. Moreover, the fluorescence "Off–On–Off " switching response of probe **10** in the presence of two chemical inputs, in the form of Cr^{3+} and PO_4^{3-} ions, has been utilized to construct an INHIBIT logic gate. Also probe **10** has been utilized to print secret letters through Cr^{3+} solution ink that can be decoded under UV light. Overall, the experimental observation further strengthens the designing of good sensor motif for the detection of Cr^{3+} in the solution, on printing paper and as well as in live cells.

ASSOCIATED CONTENT

*S Supporting Information

The Supporting Information is available free of charge on the ACS Publications website at DOI: 10.1021/acs.analchem. Synthetic route, photophysical data, and different spectral data (PDF)

AUTHOR INFORMATION

ORCID

Arvind Misra: 0000-0003-2716-4139

Notes

The authors declare no competing financial interest.

Authors contribution: Priya Singh and Biplob Koch have performed live cell imaging experiments.

Acknowledgments:

The authors are thankful to the Council of Scientific and Industrial Research (CSIR02(0199)/14/EMR-II), and University Grant Commission (UGC) New Delhi India for financial support and fellowships (to SKD, RCG) to carry out research works. We are also thankful to the Head, Department of Chemistry for their valuable support (through DST-FIST, DST-PURSE, CAS, UGC-UPE programs) and encouragements.

References:

(1) Zhu, H.; Fan, J.; Wang, B.; Peng, X. *Chem. Soc. Rev.* **2015**, *44*, 4337–4366.

(2) Wang, J.; Li, Y.; Patel, N.G.; Zhang, G.; Zhou, D.; Pang, Y. *Chem. Commun.* **2014**, *50*, 12258–12261.

(3) Goswami, S.; Aich, K.; Das, S.; Das, A.K.; Sarkar, D.; Panja, S.; Mondal, T.K.; Mukhopadhyay, S. *Chem. Commun.***2013**, *49*, 10739–10741.

(4) Vincent, J.B. *Proc Nutr Soc.* **2004**, *63*, 41– 47.

(5) Guhaa, S.; Lohar, S.; Banerjee, A.; Sahana, A.; Hauli, I.; Mukherjee, S.K.; Matalobos, J.S.; Das, D. *Talanta* **2012**, *91*,18–25.

(6) Chen, X.; Shen, X.Y.; Guan, E.; Liu, Y.; Qin, A.; Sun, J.Z.; Tang, B.Z. *Chem. Commun.* **2013**, *49*, 1503–1505.

(7) Barba-Bon, A.; Costero, A.M.; Gil, S.; Parra, M.; Soto, J.; Ramon, Martınez, M.; Sancenon, F. *Chem. Commun.* **2012**, *48*, 3000–3002.

(8) Mertz, W.; Schwarz, K. *Arch. Biochem. Biophys.***1955**, *58*, 504–506.

(9) Arakawa, H.; Ahmad, R.; Naoui, M.; Ali, H.; Riahi, T. *J. Biol. Chem.* **2000**, *275*, 10150–10153.

(10) Vincent, J.B. *Nutr. Rev.* **2000**, *58*, 67–72.

(11) Sahin, K.; Onderci, M.; Tuzcu, M.; Ustundag, B.; Cikim, G.; Ozercan, I.H.; Sriramoju, V.; Juturu, V.; Komorowski, J.R. *Metab., Clin. Exp.* **2007**, *56*, 1233–1240.

(12) Wang, H.; Kruszewski, A.; Brautigan, D.L. *Biochemistry* **2005**, *44*, 8167–8175.

(13) Wu, S.; Zhang, K.; Wang, Y.; Mao, D.; Liu, X.; Yu, J.; Wang, L. *Tetrahedron Lett.* **2014**, *55*, 351–353.

(14) Gambelunghe, A.; Piccinini, R.; Ambrogi, M.; Villarini, M.; Moretti, M.; Marchetti, C.; Abbritti, G.; Muzi, G. *Toxicology* **2003,** *188*, 187–195.

(15) Meibiana, Z.; Zhijiana, C.; Qing C.; Hua, Z.; Jianlina, L.; Jiliang, H. *Mutat. Res., Genet. Toxicol. Environ. Mutagen.* **2008**, *654*, 45–51.

(16) Danadevi, K.; Rozati, R.; Banu, B.S.; Grover, P. *Mutagenesis* **2004**, *19*, 35–41.

(17) Gomez, V.; Callao, M.P. *TrAC, Trends Anal. Chem.* **2006**, *25*, 1006–1015.

(18) Saha, S.; Mahato, P.; Reddy G, U.; Suresh, E.; Chakrabarty, A.; Baidya, M.; Ghosh, S.K.; Das, A. *Inorg. Chem.* **2012**, *51*, 336–345.

(19) Karak, D.; Banerjee, A.; Sahana, A.; Guha, S.; Lohar, S.; Adhikari, S. S.; Das, D. *J. Hazard. Mater.* **2011**, *188*, 274–280.

(20) Mahato, P.; Saha, S.; Suresh, E.; Liddo, R.D.; Parnigotto, P.P.; Conconi, M.T.; Kesharwani, M.K.; Ganguly, B.; Das, A. *Inorg. Chem.* **2012**, *51*, 1769–1777.

(21) Peräniemi, S.; Ahlgré, M. *Anal. Chim. Acta* **1995**, *315*, 365–370.

(22) Shemirani, F.; Rajabi, M. *J. Anal. Chem.* **2001**, *371*, 1037–1040.

(23) Singh, A.K.; Gupta, V.K.; Gupta, B. *Anal. Chim. Acta* **2007**, *585*, 171–178.

(24) Kim, H.N.; Lee, M.H.; Kim, H.J.; Kim, J.S.; Yoon, J. *Chem. Soc. Rev.* **2008**, *37*, 1465–1472.

(25) Chen, X.; Pradhan, T.; Wang, F.; Kim, J.S.; Yoon, J. *Chem. Rev.* **2012**, *112*, 1910–1956.

(26) Tang, B.; Yue, T.; Wu, J.; Dong, Y.; Ding, Y.; Wang, H. *Talanta* **2004**, *64*, 955–960.

(27) Gupta, V.K.; Mergu, N.; Singh, A.K. *Sens. Actuators, B* **2015**, 220, 420–432.

(28) Goswami, S.; Das, A.K.; Maity, A.K.; Manna, A.; Aich, K.; Maity, S.; Saha, P.; Mandal, T.K. *Dalton Trans.* **2014**, *43*, 231–24.

(29) Han, Y.; You, Y.; Lee, Y.; Nam, W. *Adv. Mater.* **2012**, *24*, 2748–2754.

(30) Wu, H.; Zhou, P.; Wang, J.; Zhao, L.; Duan, C. *New J. Chem.* **2009**, *33*, 653–658.

(31) Huang, K.; Yang, H.; Zhou, Z.; Yu, M.; Li, F.; Gao, X.; Yi, T.; Huang, C.*Org. Lett.* **2008**, *10*, 2557–2560.

(32) Zhou, Z.; Yu, M.; Yang, H.; Huang, K.; Li, F.; Yi, T.; Huang, C. *Chem. Commun.* **2008**, *29*, 3387–3389.

(33) Mahato, P.; Saha, S.; Suresh, E.; Liddo, R.D.; Parnigotto, P.P.; Conconi, M.T.; Kesharwani, M.K.;Ganguly, B.; Das, A. *Inorg. Chem.* **2012**, *51*, 1769–1777.

(34) Chereddy, N.R.; Nagaraju, P.; NiladriRaju, M.V.; Krishnaswamy, V.R.; Korrapati, P.S.; Bangal, P.R.; Rao, V.J. *Biosens. Bioelectron.* **2015**, *68*, 749–756.

(35) Chereddy, N.R.; Saranraj, K.; Barui, A.K.; Patra, C.R.; Rao, V.J.; Thennarasu, S. *RSC Adv.***2014**, *4*, 24324–24327.

(36) Srivastava, P.; Ali, R.;Razi, S.S.; Shahid, M.; Patnaik, S.; Misra, A. *Tetrahedron Lett.* **2013**, *54*, 688–3693.

(37) Srivastava, P.; Razi, S.S.; Ali, R.; Gupta, R.C.; Yadav, S.S.; Narayan, G., Misra, A. *Anal. Chem.* **2014**, *86*, 8693–8699.

(38) Dwivedi, S.K.; Gupta, R.C.; Ali, R.; Razi, S.S.; Hira, S.K.; Manna, P.P.; Misra, A. *J. Photochem. Photobiol., A* **2018**, *358*, 157–166.

(39) De Silva, A.P.; Nimal Gunaratne, H. Q.; Gunnlaugsson, T.; Huxley, A. J. M.; McCoy, C. P.; Rademacher, J.T.; Rice. T.E. *Chem. Rev.***1997**, *97*, 1515–1566.

(40) De Silva, A.P.; Nimal Gunaratne, H.Q.; Gunnlaugsson, T.; Mark Lynch, P.L. *New J. Chem.* **1996**, *20*, 871–880.

(41) Speiser, S. *Chem. Rev.***1996**, *96*, 1953–1976.

(42) Gupta, R.C.; Razi, S.S.; Ali, R.; Dwivedi, S.K.; Srivastava, P.; Singh, P.; Koch, B.; Mishra, H.; Misra, A. *Sens. Actuators, B* **2017**, 251,729–738.

(43) Misra, A.; Shahid, M.; Srivastava, P. *Sens. Actuators, B* **2012**, *169*, 327–340.

(44) Benesi H.A.; Hildebrand, J. H. *J. Am. Chem. Soc.* **1949**, *71*, 2703–2707.

(45) Nayab, P.S.; Shkir, M.; *Sens. Actuators, B* **2017**, *251*, 951–957.

(46) Liu, H.; Wan, X.; Liu, T.; Li, Y.; Yao, Y. *Sens. Actuators, B* **2014**, *200*, 191–197.

(47) Saleh, F.Y.; Mbamalu, G.E.; Jaradat, Q.H.; Brungardt, C.E. *Anal. Chem.***1996**, *68*, 740–745.

For TOC only